

Attempt to confirm superheavy element production in the $^{48}\text{Ca} + ^{238}\text{U}$ reaction

K.E. Gregorich¹, W. Loveland², D. Peterson³, P.M. Zielinski^{1,4}, S.L. Nelson^{1,4}, Y.H. Chung⁵,
Ch.E. Düllmann^{1,4}, C.M. Folden III^{1,4}, K. Aleklett⁶, R. Eichler^{7,8}, D.C. Hoffman^{1,4},
J.P. Omtvedt⁹, G.K. Pang⁴, J.M. Schwantes^{4,10}, S. Soverna^{7,8}, P. Sprunger², R. Sudowe¹,
R.E. Wilson^{1,4}, and H. Nitsche^{1,4}

¹*Nuclear Science Division, Lawrence Berkeley National Laboratory, Berkeley, California 94720*

²*Department of Chemistry, Oregon State University, Corvallis, Oregon 97331*

³*Physics Division, Argonne National Laboratory, Argonne, Illinois 60439*

⁴*Department of Chemistry, University of California, Berkeley, California 94720*

⁵*Department of Chemistry, Hallym University, Chuncheon, Korea 200-702*

⁶*Department of Chemistry, Uppsala University, Uppsala, Sweden*

⁷*Labor für Radio- und Umweltchemie, Paul Scherrer Institut, CH-5232 Villigen PSI, Switzerland*

⁸*Departement für Chemie und Biochemie, Universität Bern, CH-3012 Bern, Switzerland*

⁹*Department of Chemistry, University of Oslo, Oslo, Norway*

¹⁰*Isotope & Nuclear Chemistry, Los Alamos National Laboratory, Los Alamos, New Mexico 87545*

24 March 2005

An attempt to confirm production of superheavy elements in the reaction of ^{48}Ca beams with actinide targets has been performed using the $^{238}\text{U}(^{48}\text{Ca},3n)^{283}112$ reaction. Two ^{48}Ca projectile energies were used, that spanned the energy range where the largest cross sections have been reported for this reaction. No spontaneous fission events were observed. No alpha decay chains consistent with either reported or theoretically predicted element 112 decay properties were observed. The cross section limits reached are significantly smaller than the recently reported cross sections.

PACS Number(s): 25.70.Jj, 27.90.+b

I. INTRODUCTION

During the past five years, several reports on the production of superheavy elements (SHE) in the reaction of ^{48}Ca beams with actinide targets have been published. Results from a Dubna / Livermore / Sarov collaboration, using the Dubna Gas Filled Recoil Separator (DGFRS) [1], are summarized in three recent publications [2-4] and references cited therein. Concurrent reports, published by a Dubna / Darmstadt / Bratislava / Wako collaboration, describe use of the Dubna VASSILISSA electrostatic recoil separator [5], to produce and identify SHE in the $^{238}\text{U}(^{48}\text{Ca},3n)^{283}112$ [6,7] and $^{242}\text{Pu}(^{48}\text{Ca},3n)^{287}114$ [8] reactions. Although these are two of the same nuclear reactions used in the DGFRS work, strikingly different decay properties were reported for $^{283}112$ and $^{287}114$.

If correct, these experiments represent the discovery of SHE, and have far-reaching implications for the study of the nuclear and chemical properties of the heaviest elements. We have attempted to independently confirm one of the SHE claims using the Lawrence Berkeley National Laboratory (LBNL) Berkeley Gas-filled Separator (BGS) [9]. For this confirmation attempt, the $^{238}\text{U}(^{48}\text{Ca},3n)^{283}112$ reaction was chosen as the most accessible. Targets of ^{238}U , with a relatively low specific activity, can be used with no modifications to the BGS, and the reported formation cross sections of 2.5 pb [4] and 4 pb [7] are large enough to obtain statistically significant results on a time scale of weeks.

The VASSILISSA group has reported that $^{283}112$ decays by spontaneous fission (SF) with a half-life of 5.1 minutes [7]. In the more extensive set of experiments with the DGFRS, $^{283}112$ is reported to decay by emission of 9.54-MeV α -particles with a half-life of 4.0 s [4]. The DGFRS group also reports that the ^{279}Ds daughter decays predominantly by SF with a 0.18-s half-life. All reported SHE decay chains terminate with SF decay.

II. EXPERIMENT

$^{48}\text{Ca}^{10+}$ beams were accelerated by the LBNL 88-Inch Cyclotron to laboratory-frame energies of 243.5 MeV and 248.3 MeV. At the entrance to the BGS, the beam passed through a 0.045 mg/cm^2 carbon vacuum window before entering the targets. Targets consisted of 0.58 mg/cm^2 Al foils with $^{238}\text{UF}_4$ evaporated onto the downstream side. Nine of these targets on arc-shaped frames were arranged at the periphery of a 35-cm diameter wheel which was rotated at ~ 500 RPM. Several sets of targets were used during the course of these experiments. The different target sets had average UF_4 thicknesses between 0.48 mg/cm^2 and 0.61 mg/cm^2 , as indicated in Table 1. ^{48}Ca stopping powers were calculated with SRIM2003 [10]. In the irradiation with the 243.5-MeV beam, the ^{48}Ca energy entering the UF_4 layer was 233.2 MeV, and the average energy exiting the UF_4 was between 227.2 and 228.5 MeV. The beam-dose-weighted average center-of-target (COT) energy was 230.3 MeV. (Hereafter, this will be referred to as the 230.3-MeV irradiation.) The 230.3-MeV irradiation result reported here includes previously published data [11], and an additional experiment carried out under nearly identical conditions. For the higher energy irradiation with the 248.3-MeV beam, the ^{48}Ca energy entering the target was 238.0 MeV, and the average energy exiting the targets was between 232.5 and 233.5 MeV. The beam-dose-weighted average COT energy was 235.6 MeV. (Hereafter, this will be referred to as the 235.6-MeV irradiation.) Using experimental mass excesses [12] for ^{48}Ca and ^{238}U , and a calculated value [13,14] for $^{286}112$, the COT excitation energies are 31.9 MeV and 36.3 MeV, for the 230.3-MeV and 235.6-MeV irradiations, respectively. Typical ^{48}Ca beam intensities were $\sim 3 \times 10^{12}$ ions/s. The product of beam intensity and target thickness was recorded continuously with two Si p-i-n diode “monitor detectors” mounted at $\pm 27^\circ$ from the incident beam direction that detected ^{48}Ca beam particles elastically scattered from ^{238}U target atoms. Attenuating screens were installed in front of these monitor detectors to reduce the number of particles reaching them (and consequent radiation damage to the detectors). Irradiation parameters are summarized in Table 1.

Compound nucleus evaporation residues (EVRs) would be formed in the UF_4 target with the momentum of the beam, and a kinetic energy of approximately 39 MeV. The BGS was filled with He gas at 66 Pa (93 Pa for the 230.3-MeV irradiation). EVRs were spatially separated from beam particles and transfer reaction products by their differing magnetic rigidities in the Berkeley Gas-filled Separator (BGS). Ghiorso *et al.* [15] have measured the magnetic rigidity of heavy ions passing through dilute He gas, and showed the general trend: $\bar{q} \propto vZ^{1/3}$, where \bar{q} is the average charge, v is the ion velocity, and Z is the atomic number of the ion. However, as shown in Fig. 3 of [15], there are significant deviations from the $\bar{q} \propto vZ^{1/3}$ trend due to the electronic shell effects in the stripped ions. We have taken these data [16], together with average charges for $Z = 99-111$ heavy ion EVRs measured in the BGS, and made a global fit to the average charge in He gas, including a sinusoidal correction for the shell structure of the stripped ion.

$$\bar{q} = mx + b + d \sin \left[\frac{2\pi}{32} (Z - (mx + b) - f) \right] \quad x = \frac{v}{v_0} Z^{1/3} \quad \text{for } Z \gtrsim 45 \quad (1)$$

$v_0 = 2.1877 \times 10^7$ m/s is the Bohr velocity. The best fit was obtained with $m = 0.641$, $b = -0.235$, $d = 0.517$, and $f = 74.647$. The first two terms in equation (1) show a linear $vZ^{1/3}$ trend, with a small zero intercept. The sinusoidal correction is based on an estimate of the number of electrons, $Z - (mx + b)$, remaining on the ion. It has an amplitude, $d = 0.517$, of approximately one half of a charge unit, and a period of 32, the length of the sixth and seventh rows of the periodic table. There is an ascending node at $f = 74.647$, about halfway through the 5d electron shell, similar to that indicated in fig. 3 of [15]. The fit in the region $9 < x < 14$, shown in Fig. 1, is especially good, with a standard deviation of 0.10 charge units. For all points, x has been determined from the energies of EVRs as they are produced at the center of the targets (\bar{q} is nearly inversely proportional to v , so the magnetic rigidities, $B\rho = mv/\bar{q}$ where m is the EVR mass, are nearly independent of velocity or energy). $^{283}\text{112}$ EVRs with a kinetic energy of 39 MeV would have $x = 11.30$ and $\bar{q} = 6.845 \pm 0.10$. The resulting magnetic rigidity is 2.22 ± 0.03 Tm. The BGS magnetic dispersion is $1.8 \text{ cm} / \% B\rho$. The 12-cm wide focal plane detector with a 10-cm wide parallel plate avalanche counter (PPAC) used in the 230.3-MeV irradiation spanned 2.19-2.31 Tm. The 18-cm wide focal plane detector with a 16-cm wide multiwire proportional counter (MWPC) used in the 235.6-MeV irradiation spanned 2.11-2.31 Tm. The size of the focal plane position distribution of $^{283}\text{112}$ EVRs in the dispersive (horizontal) direction is expected to be similar to that for ^{252}No EVRs from the $^{48}\text{Ca} + ^{206}\text{Pb}$ reaction. The ^{252}No horizontal position distribution is roughly Gaussian with a full-width-at-half-maximum (FWHM) of 7 cm.

The efficiency for collecting $^{283}\text{112}$ EVRs at the BGS focal plane was estimated using a combination of experimentally measured efficiencies, together with a Monte Carlo simulation of the EVR trajectories in the BGS, as described earlier [11,17]. Separator efficiency for the 230.3-MeV irradiation was 49%. With increased detector size, slightly lower He gas pressure, and a smaller vertical target size, the efficiency was increased to 59% for the 235.6-MeV irradiation.

Ions arriving at the focal plane region of the BGS passed through a veto detector used to distinguish beam-related particles hitting the focal plane Si-strip detector from events due to the decay of previously implanted atoms. A $10 \text{ cm} \times 10 \text{ cm}$ PPAC [18] with a thickness equivalent to 0.6 mg/cm^2 carbon was used together with the previously-described [11,17] $12 \text{ cm} \times 6 \text{ cm}$ Si strip array for the 230.3-MeV irradiation. For the 235.6-MeV irradiation, an expanded focal plane detector array was used, consisting of a $16 \text{ cm} \times 8 \text{ cm}$ MWPC [19] with a thickness equivalent to 0.5 mg/cm^2 carbon and an $18 \text{ cm} \times 6 \text{ cm}$ Si-strip array [20]. The PPAC and the MWPC were run with isobutane at a pressure of 500 Pa. The focal plane detector contained 48 3.75-mm wide strips (32 strips for the 230.3-MeV irradiation). Horizontal positions were provided by the strip number identification. Vertical positions were determined by resistive charge division. Both Si-strip arrays included “upstream detectors” in a five-sided box configuration (left and right sides of the box were omitted for the 230.3-MeV irradiation), as well as a second set of Si-strip “punchthrough detectors” located directly behind the focal plane detectors. These upstream and punchthrough detectors had adjacent sets of four strips galvanically connected, resulting in 32 upstream detector segments (16 upstream detector segments for the 230.3-MeV irradiation) and 12 punchthrough detector segments. Data were

recorded in list mode. Any event depositing > 300 keV (> 500 keV for the 230.3 MeV irradiation) in the focal plane Si-strip detector, or > 1 MeV in the upstream detector box triggered data acquisition. Pulse amplitudes were recorded from the top and bottom of the focal plane strips (two gain ranges: 0-20 MeV and 0-200 MeV), from the upstream detector strips (two gain ranges: 0-20 MeV and 0-200 MeV), from the punchthrough detector strips (0-20 MeV), and from the PPAC or MWPC, together with the time from a 1 MHz oscillator and a time-to-amplitude converter between the PPAC or MWPC and the focal plane detector. An additional trigger was used to record energy and time of events in the Rutherford monitor detectors. With the use of buffering ADCs and scalers, the minimum time between events was $15 \mu\text{s}$ for the 230.3-MeV irradiation and $11 \mu\text{s}$ for the 235.6-MeV irradiation.

The α -particle energy resolution in the focal plane detector was 50 keV FWHM. For α -particles escaping the focal plane detector and depositing their residual energy in the upstream strips, the reconstructed energy resolution was approximately 100 keV FWHM. The α -particle detection efficiency, including events with energies reconstructed from signals in the upstream detectors was approximately 75% (73% for the 230.3-MeV irradiation). The vertical position resolution was measured using α - α correlations from $^{252}\text{No} - ^{248}\text{Fm}$ decays produced in a $^{206}\text{Pb}(^{48}\text{Ca}, 2n)^{252}\text{No}$ test experiment. The energy dependence of the position resolution was determined by error propagation techniques, and can be approximated by $\sigma_y(E) = 2800 \text{ keV}\cdot\text{mm} / E$. Because of uncertainties in extrapolating to the low gain (0-200 MeV) energy calibrations, the vertical position uncertainty, $\sigma_y(E)$, used in data analysis was increased by 1.5 mm for any vertical positions determined from the low-gain signals.

To estimate the EVR energies entering the Si-strip detector, stopping powers in the UF_4 target material and in the He gas were estimated with SRIM2003 [10] by calculating stopping powers for $A=283$ ions from $Z=33-90$, and extrapolating as a function of $Z^{2/3}$. The resulting energies after passing through remaining target material and the He gas fill in the BGS are between 27 and 39 MeV. To estimate the $^{283}\text{112}$ energy loss in the PPAC or MWPC detectors, and the resulting energy at the focal plane Si-strip detector, the residual range technique was used. $^{283}\text{112}$ ranges were determined with SRIM2003 [10] by calculating ranges for $A=283$ ions from $Z=33-90$ and extrapolating as a function of $Z^{-2/3}$. This procedure resulted in expected $^{283}\text{112}$ energies entering the focal plane Si-strip detectors between 7.5 and 19.5 MeV. Applying pulse-height defects according to Moulton [21] gives expected EVR pulse heights corresponding to 2.3-8.1 MeV.

III. RESULTS AND DISCUSSION

In addition to the 230.3-MeV irradiation described previously [11], this paper reports results from a new 230.3-MeV irradiation that was carried out under very similar experimental conditions in 2002, and the 235.6 MeV irradiation that was performed in 2004. For the 235.6-MeV irradiation, at a typical beam intensity of $\sim 3 \times 10^{12}$ ions/s, the overall event rate (> 0.3 MeV in the focal plane Si-strip detector) was approximately 8 Hz. The rate of α -particle like events (energy in the focal plane detector between 7 and 14 MeV, with no above threshold signal in the punchthrough or MWPC) was 0.04 Hz. The rate of EVR-like events (energy in the focal plane detector between 2 and 16 MeV, with a valid MWPC hit, and no above-threshold punchthrough detector signal) was 0.7 Hz. Rates in the 230.3-MeV irradiations, with the smaller focal plane detector, were slightly lower.

According to theoretical predictions [22] and the published claims [3,4,6,7], production of SHE in the region of $^{283}112$ should result in SF decay of either the produced isotope, or one of the daughter isotopes. This experiment was sensitive to SF decays with lifetimes from 11 μs (15 μs for the 230.3-MeV irradiation) to approximately 10^6 seconds. In our off-line searches, the signature for a SF event was a pulse height in the focal plane detector with an amplitude greater than 96 MeV, with no coincident signal above threshold in the MWPC (PPAC). 95% of the SF signals from the decay of ^{252}No produced in the $^{208}\text{Pb}(^{48}\text{Ca},2n)^{252}\text{No}$ test reaction lie above this 96-MeV threshold. SF of $Z \geq 110$ isotopes is expected to have significantly higher fragment energies. In all of the $^{48}\text{Ca} + ^{238}\text{U}$ experiments combined, there were 324 events exceeding this energy threshold, all of which had distinct MWPC or PPAC signals (9 of the events in the 230.3-MeV irradiation had large amplitude signals in all focal plane strips, and were presumably caused by sparking of the PPAC). High energy focal plane events coincident with signals in the MWPC or PPAC are indicative of scattered beam passing through the BGS. From the focal plane detector, the MWPC (PPAC) subtended only $\sim 2\%$ of 4π sr. Thus only $\sim 4\%$ of true SF events are expected to include MWPC or PPAC signals (this number is confirmed in the $^{206}\text{Pb}(^{48}\text{Ca},2n)^{252}\text{No}$ test experiments). **No SF events were observed in any of the $^{48}\text{Ca} + ^{238}\text{U}$ irradiations.**

Table 1 summarizes the irradiations and cross section limits reached. The simple “one-event” cross section limits listed in the sixth column of Table 1 are the cross sections which would have been reported if a single event were observed, assuming a constant cross section at all beam energies within the target. In the seventh column of Table 1, the cross section upper limits for an 84% confidence level are reported. The limit for an 84% confidence level is similar to the usual one-sigma upper limit, with 16% of the probability lying above this limit. These 84% confidence level limits include a Poisson treatment of counting statistics [23], as well as a 12% systematic uncertainty. The cross section limits listed in the sixth and seventh columns of Table 1 are for the magnetic rigidities at which each experiment was optimized (2.25 Tm and 2.21 Tm for the 230.3- and 235.6-MeV irradiations, respectively). However, the sensitivity of our experiments depends on the true magnetic rigidity of element 112 recoils in the He gas. Column 8 of Table 1 lists the maximum 84% confidence level upper cross section limits within \pm one sigma of the expected magnetic rigidity (also including the 12% systematic uncertainty).

The systematic uncertainties result from five main contributions: 1) The uncertainty in the efficiency for transport of EVRs to the focal plane detector array is uncertain by approximately $\Delta_{\text{eff}}/\text{eff} = 10\%$. 2) A 0.2° uncertainty in the average angle of the Rutherford monitor detectors with respect to the beam direction results in a 3% uncertainty in the Rutherford scattering cross section, and a corresponding 3% uncertainty in EVR cross sections. 3) The uncertainty in the solid angle subtended by the collimators placed in front of the monitor detectors is dominated by uncertainty in the size of the opening, and is estimated to contribute 4% to the systematic error in cross sections. 4) The attenuation factors of the screens between the target and monitor detectors have been measured with the $^{207}\text{Pb}(^{48}\text{Ca},2n)^{253}\text{No}$ reaction. The ratio of ^{253}No EVRs in the BGS focal plane detector to Rutherford scattered ^{48}Ca ions in the monitor detectors was measured with and without the attenuation screens. The uncertainty in this attenuation factor is 5%. 5) The absolute energy from the 88-Inch Cyclotron is known to an accuracy of approximately 1% . The energy loss calculation in the carbon vacuum window, aluminum target backing, and UF_4 layer has been shown to be accurate to approximately 1.0 MeV. The resulting beam energy uncertainty is 2.6 MeV. This has a 2% effect on the Rutherford scattering cross section, and thus contributes a 2% uncertainty to the cross sections

measured in the BGS. Standard error propagation of these five contributions results in an overall systematic uncertainty of 12% for cross sections (or cross section limits) measured with the BGS.

Searches for possible element 112 decay chains which are not terminated by SF (or where the SF lifetime is longer than the duration of our experiment) have also been performed. **No EVR- α - α correlations with $\Delta t(\text{EVR-}\alpha) < 20$ s and $\Delta t(\alpha\text{-}\alpha) < 20$ s were observed in any of the $^{48}\text{Ca} + ^{238}\text{U}$ irradiations.** For these searches, EVRs were defined as focal plane events with recorded energies between 6 and 16 MeV (2 to 12 MeV for the 230.3-MeV irradiation, with the thicker PPAC) coincident with MWPC (PPAC) signals, and anticoincident with any above-threshold punchthrough detector signals. Alpha events were required to have $8 < E(\text{MeV}) < 11$ (focal plane only, or energies reconstructed from the sum of focal plane and upstream detectors), anticoincident with the MWPC (PPAC) and punchthrough detectors. In all searches, the EVR- α position window was $\pm 3(\sigma(E_{\text{EVR}})^2 + \sigma(E_{\alpha 1})^2)^{1/2}$ and the α - α position window was $\pm 3(\sigma(E_{\alpha 1})^2 + \sigma(E_{\alpha 2})^2)^{1/2}$. Alpha decay chains similar to those predicted [24] or those reported [4] have $^{283}112$, ^{279}Ds , and ^{275}Hs half-lives significantly shorter than the 20-s time windows. With our 75% α -particle detection efficiency, the probability of detecting an EVR followed by at least two of these three α -decays is $\sim 84\%$. Cross section limits for postulated element 112 decay chains not terminated by SF are larger than those reported in Table 1 by a factor of $1/0.84 = 1.19$.

A more stringent cross section upper limit can be obtained from these data by combining the results from the irradiations at the two ^{48}Ca beam energies. The excitation function for the $^{238}\text{U}(^{48}\text{Ca}, 3n)^{283}112$ reaction is expected to be broad [3,4]. Simulations of the $^{283}112$ detection rates in the BGS for assumed Gaussian excitation functions with FWHM = 6.6 MeV were performed in a manner similar to those reported earlier [17]. These calculations indicate significant energy overlap between the 230.3- and 235.6-MeV irradiations. A contour plot of the cross section limits reached in our *combined* experiments at an 84% confidence level is presented in Fig. 2, as a function of both the assumed excitation function centroid and assumed $^{283}112$ magnetic rigidity. These cross section limits include a Poisson treatment of the counting statistics [23] as well as a 12% systematic error. The crosses in Fig. 2 indicate the average ^{48}Ca beam energy widths in the targets and the magnetic rigidity ranges covered by the detector arrays.

The Dubna Gas-Filled Recoil Separator group has reported a cross section of 2.5 pb at 234 MeV based on six events [4]. The cross section limits presented in Fig. 2 indicate a significant discrepancy between this work and that reported by the DGFRS group.

A statistical analysis has been performed to quantify the possibility that the element 112 production cross section discrepancy could be due to counting statistics. The Poisson distribution,

$$p(N, Y) = Y^N e^{-Y} / N! \quad , \quad (2)$$

gives the statistical probability, p , to observe N events when the true rate would result in Y events. Assuming the DGFRS report of six events is correct,

$$P_{\text{DGFRS}}(Y_{\text{DGFRS}}) = p(6, Y_{\text{DGFRS}}) \quad (3)$$

describes the probability distribution for different values of Y_{DGFRS} . Here, Y_{DGFRS} is the number of events expected in the DGFRS experiment at 234 MeV for different assumed *true* production rates. This true event number distribution was then scaled by the relative sensitivities of the DGFRS and BGS experiments and normalized, to give a probability distribution of numbers of events expected in the present work,

$$P(Y_{BGS}) = p(6, Y_{BGS} \cdot L_{DGFRS}/L_{BGS}) L_{DGFRS}/L_{BGS} \cdot \quad (4)$$

Here, the sensitivity of an experiment, L , is the expected number of events per picobarn of cross section. Finally, the probability of observing zero events in the present work was determined by integrating the Poisson probability for observing zero events over the distribution of expected numbers of events in this work:

$$P_{zero} = \int_0^{\infty} P(Y_{BGS}) \cdot p(0, Y_{BGS}) dY_{BGS} \cdot \quad (5)$$

This procedure was carried out with the L_{BGS} for each point in the data set underlying the contour plot in Fig. 2, and the results are presented in Fig. 3a. The contours as labeled in Fig. 3a show the probability, based on counting statistics, of observing zero events in the present work, assuming the DGFRS observation of six events at 2.5 pb is correct. This calculation ignores *differences* in systematic errors between the two experiments. Differences in systematic errors are discussed below. $^{283}112$ is expected to be produced with a roughly Gaussian excitation function. DGFRS results indicate the centroid, c , to be near 234 MeV [4]. At the expected magnetic rigidity of 2.22 Tm, this calculation indicates only a 2% statistical probability of obtaining our null result. This probability remains below 10% over the region spanning $c = 234 \pm 3$ MeV and $\pm 2\sigma$ from the expected magnetic rigidity.

Two of the six $^{238}\text{U}(^{48}\text{Ca},3n)^{283}112$ decay sequences reported by the DGFRS group at the ^{48}Ca beam energy of 234 MeV consist of EVR-SF correlations (the 9.54-MeV α -decay assigned to $^{283}112$ was not recorded [4]). One could assume that these two EVR-SF events are random correlations between EVR-like signals and background SF events. The calculations for Fig. 3a have been repeated under the corresponding assumption of a DGFRS cross section of 1.67 pb based on observation of four $^{283}112$ events. The results of this revised calculation are plotted in Fig 3b. Even after excluding two of the six DGFRS $^{283}112$ events, we find only a 6% statistical probability of obtaining our null result at the expected values of $c = 234$ MeV and magnetic rigidity = 2.22 Tm. This probability remains below 20% over the region spanning $c = 234 \pm 3$ MeV and $\pm 2\sigma$ from the expected magnetic rigidity.

To examine whether the disagreement between this work and that in reference [4] could be due to differences in beam energies from the two accelerators, absolute beam energies from the 88-Inch Cyclotron and the Dubna U400 Cyclotron have been compared using the excitation functions for $^{208}\text{Pb}(^{48}\text{Ca},2n)^{254}\text{No}$ reactions carried out at both accelerators [25-28]. ^{254}No excitation functions for the DGFRS and VASSILISSA at the Dubna U400 Cyclotron, and for the BGS at the LBNL 88-Inch Cyclotron are plotted in Fig. 4. Fits were performed on the data from each of the separators, employing a Gaussian smoothly joined to an exponential tail on the high-energy side:

$$\zeta = Ae^{-(E-c)^2/2w^2}, E \leq \lambda w^2 + c \quad \zeta = Ae^{\lambda w^2/2} e^{-\lambda(E-c)}, E > \lambda w^2 + c \quad (6)$$

where ζ is the cross section as a function of the ^{48}Ca beam energy, E . A is the amplitude at the centroid, c , of a Gaussian with width, w , and λ is the exponential slope. All exponential slopes were fixed a $\lambda = 0.41 \text{ MeV}^{-1}$, the value favored by the VASSILISSA data. The widths of the Gaussians were allowed to vary, resulting in $w = 2.5 \text{ MeV}$ and 3.4 MeV , for the BGS and VASSILISSA, respectively. The w for the DGFRS data was fixed at the 3.4-MeV VASSILISSA value. The broader excitation functions measured at Dubna can be explained by a larger energy spread in the beams entering the targets. Centroids of the excitation functions agree to within 2.4 MeV, leading to the conclusion that the energies of beams from the two accelerators are well matched. The centroids of the BGS and DGFRS excitation functions agree to better than 1 MeV.

The energy loss calculation used to determine the ^{48}Ca beam energies in the ^{238}U targets for this work has been compared to that in $\text{Ca} + \text{Pb}$ reactions by measuring the pulse-heights from Rutherford-scattered ^{48}Ca ions in the beam monitor detectors. A comparison of the monitor detector pulse amplitudes from the $^{48}\text{Ca} + ^{207}\text{Pb}$ test reaction (where the energy loss calculation is assumed to be accurate due to the thin C target backings and well-characterized, uniform ^{207}Pb layer) with those from the $^{48}\text{Ca} + ^{238}\text{U}$ reactions of this experiment indicates that the energy loss calculation is accurate to within approximately 1 MeV. The reproducibility of beam energies from temporally separated experiments at the 88-Inch Cyclotron was determined by measuring the beam energy spectrum in a Si p-i-n diode for 7 different ^{48}Ca beam energies between 203 and 219 MeV. Deviations from the expected linear relationship between pulse-height recorded in the p-i-n diode and the square of the cyclotron frequency gave a standard deviation of 0.2% (FWHM = 0.5%) for the beam energy.

Fig. 4 can also be used to assess the differences in possible systematic errors affecting the sensitivities of the three separators. The heights of the three excitation functions agree to within a factor of 1.6. The heights of the BGS and DGFRS excitation functions agree to within a factor of 1.2. Taking the relative heights of the excitation functions in Fig 4. at face value indicates that systematic error effects result in slightly larger detection rates near the centroid of the excitation function in the BGS than in the DGFRS. This would make the discrepancy in experimental results between these experiments and those from the DGFRS slightly larger than indicated in Fig. 3.

All heavy element decay chains in the region of N and Z near $^{283}112$ are expected to terminate with SF. Because of the large angular acceptance of the BGS, efficiencies for compound nucleus formation with charged-particle exit channels remains large. Our data exclude SHE formation in reactions such as $^{238}\text{U}(^{48}\text{Ca},\text{pxn})^{285-x}111$, and $^{238}\text{U}(^{48}\text{Ca},\alpha\text{xn})^{282-x}110$ at cross section limits only slightly larger than those presented in Fig. 2.

In summary, we have been unable to reproduce the Dubna results, either from VASSILISSA or DGFRS, for superheavy element production in the $^{48}\text{Ca} + ^{238}\text{U}$ reaction over a generous range of projectile energies and assumed element SHE magnetic rigidities.

Acknowledgement

We gratefully acknowledge the operations staff of the 88-Inch Cyclotron for providing the intense beams of ^{48}Ca . ^{207}Pb targets were provided by the GSI target laboratory. Financial support was provided by the Office of High Energy and Nuclear Physics, Nuclear Physics

Division of the U.S. Department of Energy, under contract DE-AC03-76SF000988 and grant DE-FG06-97ER41026, the Swiss National Science Foundation, the Norwegian Research Council project No. 138507/410, and the Swedish Foundation for International Cooperation in Research and Higher Education.

- [1] K. Subotic, Yu.Ts. Oganessian, V.K. Utyonkov, Yu.V Lobanov, F.Sh. Abdullin, A.N. Polyakov, Yu.S. Tsyganov, O.V. Ivanov, Nucl. Instrum. Methods Phys. Res. A **481**, 71 (2002).
- [2] Yu.Ts. Oganessian *et al.*, Phys. Rev. C **69**, 021601 (2004).
- [3] Yu.Ts. Oganessian *et al.*, Phys. Rev. C **69**, 054607 (2004).
- [4] Yu.Ts. Oganessian *et al.*, Phys. Rev. C **70**, 064609 (2004).
- [5] A.V. Yeremin *et al.*, Nucl. Instrum. Methods Phys. Res. A **350**, 608 (1994).
- [6] Yu.Ts. Oganessian *et al.*, Eur. Phys. J. A **5**, 63 (1999).
- [7] Yu.Ts. Oganessian *et al.*, Eur Phys. J. A **19**, 3 (2004).
- [8] Yu.Ts. Oganessian *et al.*, Nature **400**, 242 (1999).
- [9] V. Ninov, K.E. Gregorich, in *ENAM 98, Exotic Nuclei and Atomic Masses*, edited by B. Sherrill, D.J. Morrissey, and C.N. Davids, AIP Conf. Proc. No. 455 (AIP, Woodbury, 1998), p. 704.
- [10] www.srim.org
- [11] W. Loveland, K.E. Gregorich, J.B. Patin, D. Peterson, C. Rouki, P.M. Zielinski, K. Aleklett, Phys. Rev. C **66**, 044617 (2002).
- [12] G. Audi, A.H. Wapstra, C. Thibault, Nucl. Phys. A **729**, 337 (2003).
- [13] W.D. Myers, W.J. Swiatecki, Nucl. Phys. A **601**, 141 (1996).
- [14] W.D. Myers, W.J. Swiatecki, Lawrence Berkeley National Laboratory Report, LBNL-36803 (1994). <http://ie.lbl.gov/txt/ms.txt>
- [15] A. Ghiorso, S. Yashita, M.E. Leino, L. Frank, J. Kalnins, P. Armbruster, J.-P. Dufour, P.K. Lemmertz, Nucl. Instrum. Methods Phys. Res. A **269**, 192 (1988).
- [16] P. Armbruster, private communication containing data on heavy ion recoil charges in He gas.
- [17] K.E. Gregorich, *et al.*, Eur. Phys. J. A **18**, 633 (2003).
- [18] D. Swan, J. Yurkon, D.J. Morrissey, Nucl. Instrum. Methods Phys. Res. A **348**, 314 (1994).
- [19] M.M. Fowler *et al.*, Nucl. Instrum. Methods Phys. Res. A **281**, 517 (1989).
- [20] C.M. Folden III, K.E. Gregorich, Ch.E. Düllmann, H. Mahmud, G.K. Pang, J.M. Schwantes, R. Sudowe, P.M. Zielinski, H. Nitsche, D.C. Hoffman, Phys. Rev. Lett. **93**, 212702 (2004).
- [21] J.B. Moulton, J.E. Stephens, R.P. Schmidt, G.J. Wozniak, Nucl. Instrum. Methods Phys. Res. **157**, 325 (1978).
- [22] R. Smolańczuk, J. Skalski, A Sobiczewski, Phys. Rev. C **52**, 1871 (1995).
- [23] K.-H. Schmidt, C.-C. Sahm, K. Pielenz, H.-G. Clerc, Z. Phys. A **316**, 19 (1984).
- [24] R. Smolańczuk, Phys. Rev. C **56**, 812 (1997).
- [25] J.B. Patin, Ph.D. Dissertation, Lawrence Berkeley National Laboratory Report, LBNL-49593 (2002).
- [26] A.V. Belozarov *et al.*, Eur. Phys. J. A **16**, 447 (2003).
- [27] Yu.Ts. Oganessian *et al.*, Phys. Rev. C **64**, 054606 (2001).
- [28] A.V. Yeremin *et al.*, JINR Rapid Commun. No. **6[92]-98**, 21 (1998).

Table 1. Irradiation parameters and cross section upper limits for $^{48}\text{Ca} + ^{238}\text{U}$ experiments.

^{48}Ca energy at center of target (MeV) ^a	avg. UF ₄ thickness (μg/cm ²) ^b	^{48}Ca energy range in tgt. (MeV) ^a	$^{286}\text{112}$ excitation energy (MeV) ^c	^{48}Ca beam dose (x10 ¹⁸) ^d	simple “one-event” cross section upper limit (pb) ^e	cross section upper limit at 84% confidence level (pb) ^f	largest 84% c. l. cross section limit within ± 1σ of expected Bρ (pb) ^g
230.2 ^h	611	227.2-233.2	29.3 – 34.2	1.10	1.60		
230.8	475	228.5-233.2	30.4 – 34.2	0.27	8.18		
230.3	580	227.5-233.2	29.6 – 34.2	0.89	2.01		
230.3 dose-weighted average	583 dose-weighted average	227.5-233.2 dose-weighted average	31.9 dose-weighted average	2.26 total dose 230.3 MeV irradiation	0.80ⁱ combined limit 230.3 MeV, Bρ=2.25 Tm	1.6ⁱ combined limit 230.3 MeV, Bρ = 2.25 Tm	2.9 combined limit 230.3 MeV, Bρ=2.22±0.03
235.7	475 ^j	233.5-238.0	34.6 – 38.3	1.59	1.20		
235.2	580	232.5-238.0	33.8 – 38.3	0.26	6.07		
235.6 dose-weighted average	490 dose-weighted average	233.4-238.0 dose-weighted average	36.3 dose-weighted average	1.85 total dose 235.6 MeV irradiation	0.96 combined limit 235.6 MeV, Bρ = 2.21 Tm	2.0 combined limit 235.6 MeV, Bρ = 2.21 Tm	2.2 combined limit 235.6 MeV, Bρ=2.22±0.03

^a Laboratory frame energies. Energy loss calculated with SRIM2003 [10].

^b Thickness determined by mass, α-particle energy loss, and ^{238}U activity measurements.

^c Experimental masses for ^{48}Ca and ^{238}U used. For $^{286}\text{112}$, mass excess used from [13,14].

^d From ^{48}Ca Rutherford scattering at 27° from beam direction, with column 2 target thickness.

^e Cross section that would be reported if one event had been observed, assuming an equal production cross section at all ^{48}Ca energies in the targets. Limits are for the magnetic rigidity at which the experiments were optimized.

^f Similar to a one-sigma upper limit on a normal probability distribution, where 16% of the Poisson probability for the *true* production cross section lies above this limit. A 12% systematic uncertainty has been included. Limits are for the magnetic rigidity at which the experiments were optimized.

^g Similar the values in column 7, but the maximum limit within ± one sigma of the expected magnetic rigidity is listed.

^h This irradiation has been described in an earlier publication [11].

ⁱ “One event” and 84% confidence level upper limits at the presently favored magnetic rigidity of 2.22 Tm are 0.86 pb and 1.8 pb, respectively.

^j Targets damaged during irradiation. As in all experiments, the product of beam dose and target thickness was calculated from number of Rutherford-scattered ^{48}Ca ions.

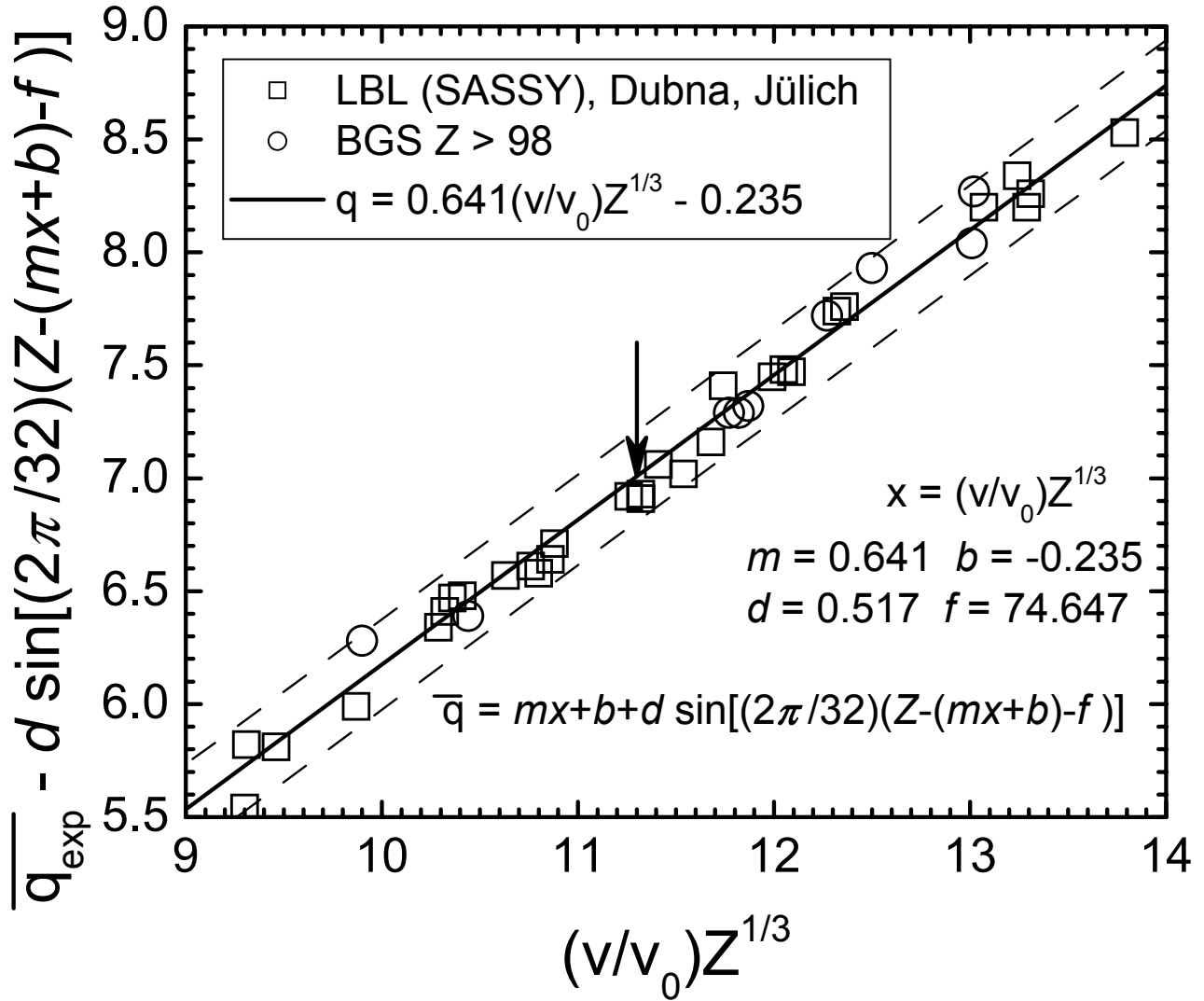


Fig. 1. Average charges of heavy ions passing through dilute He gas. The ordinate shows the experimental average charges, with the sinusoidal correction for the electronic shell structure of the stripped ions removed. The best fit is indicated by the solid line. The dashed lines indicate the $\pm 2\sigma$ deviations about the fit. The value for expected $^{283}_{112}$ EVRs is indicated with the arrow.

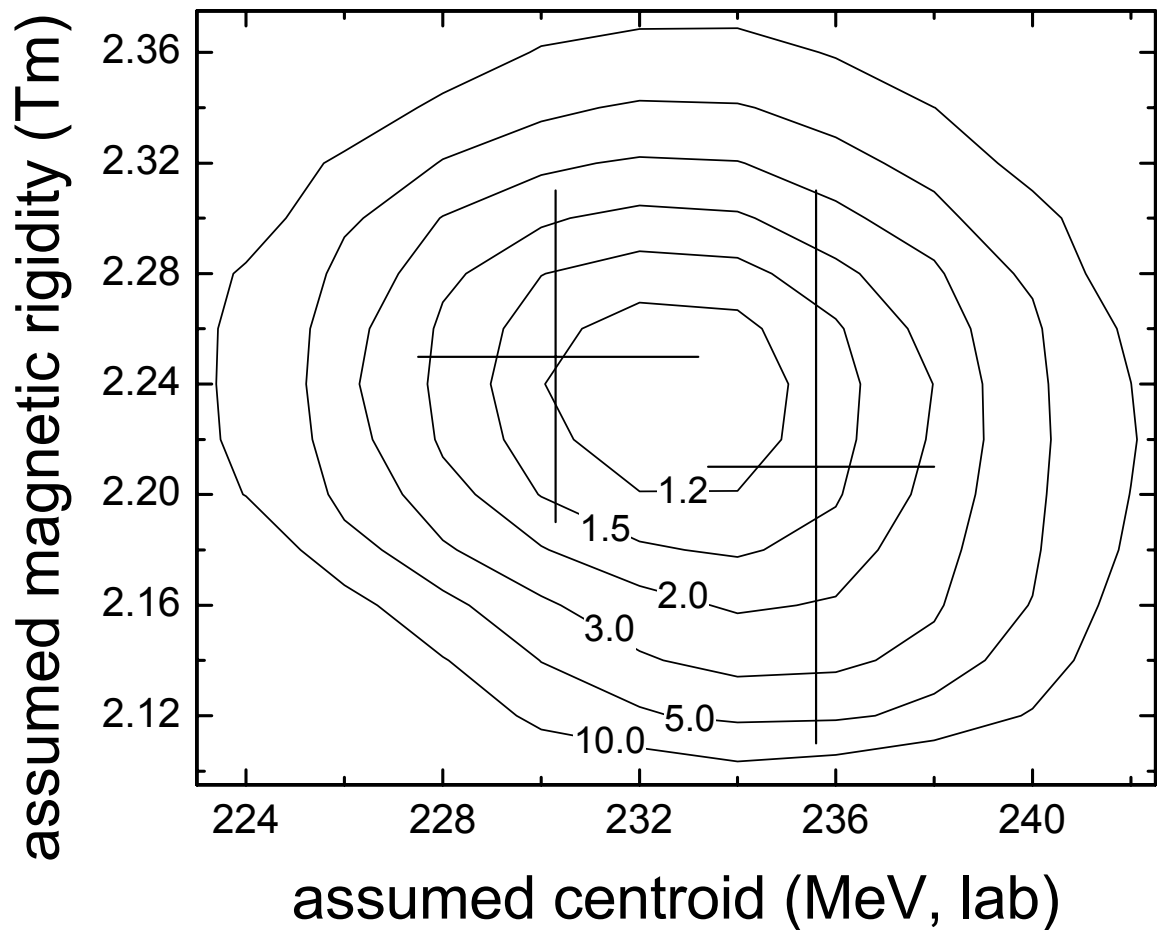


Fig. 2. Cross section limits for the combined 230.3- and 235.6-MeV irradiations shown as a function of assumed $^{283}112$ magnetic rigidity and assumed centroid for the $^{238}\text{U}(^{48}\text{Ca},3\text{n})^{283}112$ excitation function. Contours are labeled in picobarns, and represent an 84% confidence level including a Poisson treatment of counting statistics as well as a 12% systematic error. The crosses indicate ^{48}Ca beam energy ranges in the targets and focal plane detector magnetic rigidity coverage for the individual 230.3-MeV and 235.6-MeV runs.

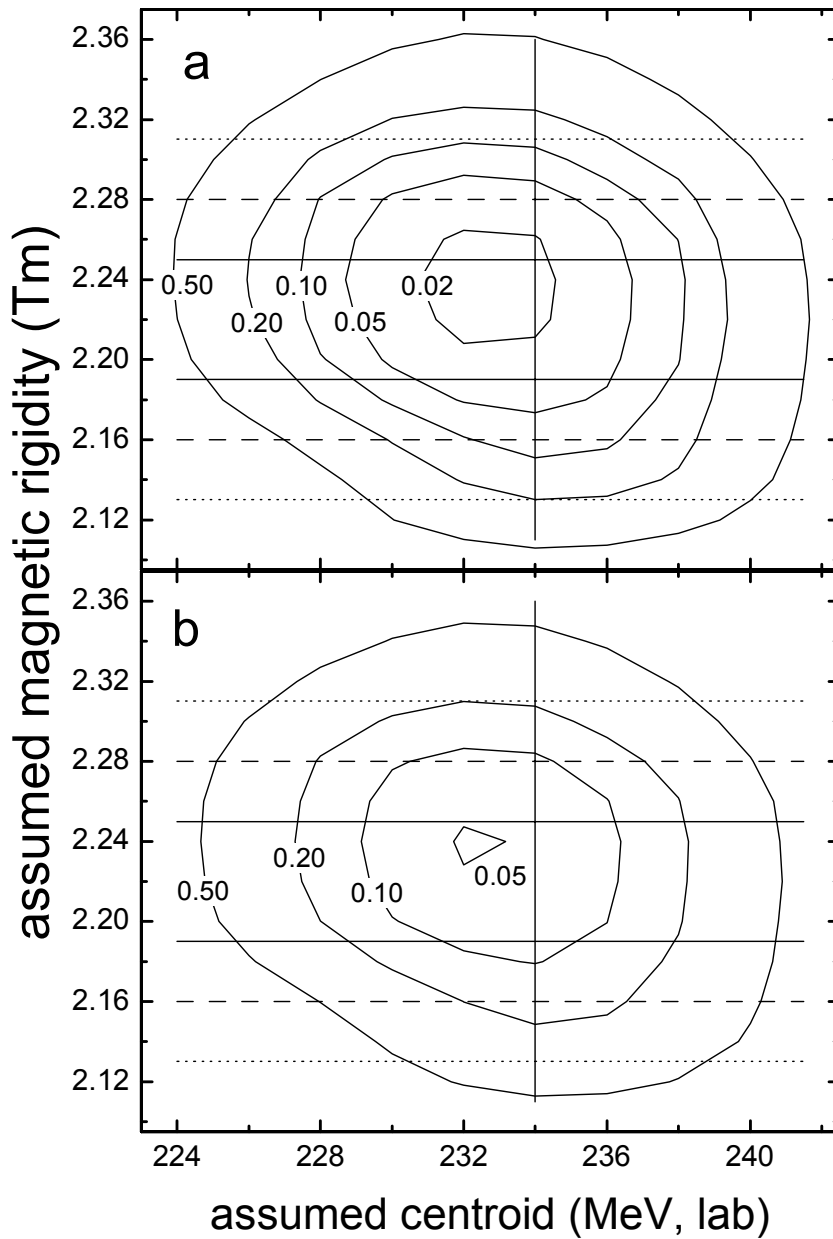


Fig. 3. a) Probability of observing zero events in the present work, assuming the reported DGFRS production rate (of 6 events at 2.5 pb) is correct, shown as a function of assumed $^{283}112$ magnetic rigidity and assumed centroid for the $^{238}\text{U}(^{48}\text{Ca},3n)^{283}112$ excitation function. This calculation considers counting statistics only, and ignores systematic errors. The vertical line indicates the reported DGFRS beam energy. Estimated 1σ , 2σ , and 3σ uncertainties in the predicted $^{283}112$ magnetic rigidity are indicated by the solid, dashed, and dotted horizontal lines, respectively. b) Same as a) with the DGFRS production rate adjusted to 4 events at 1.67 pb.

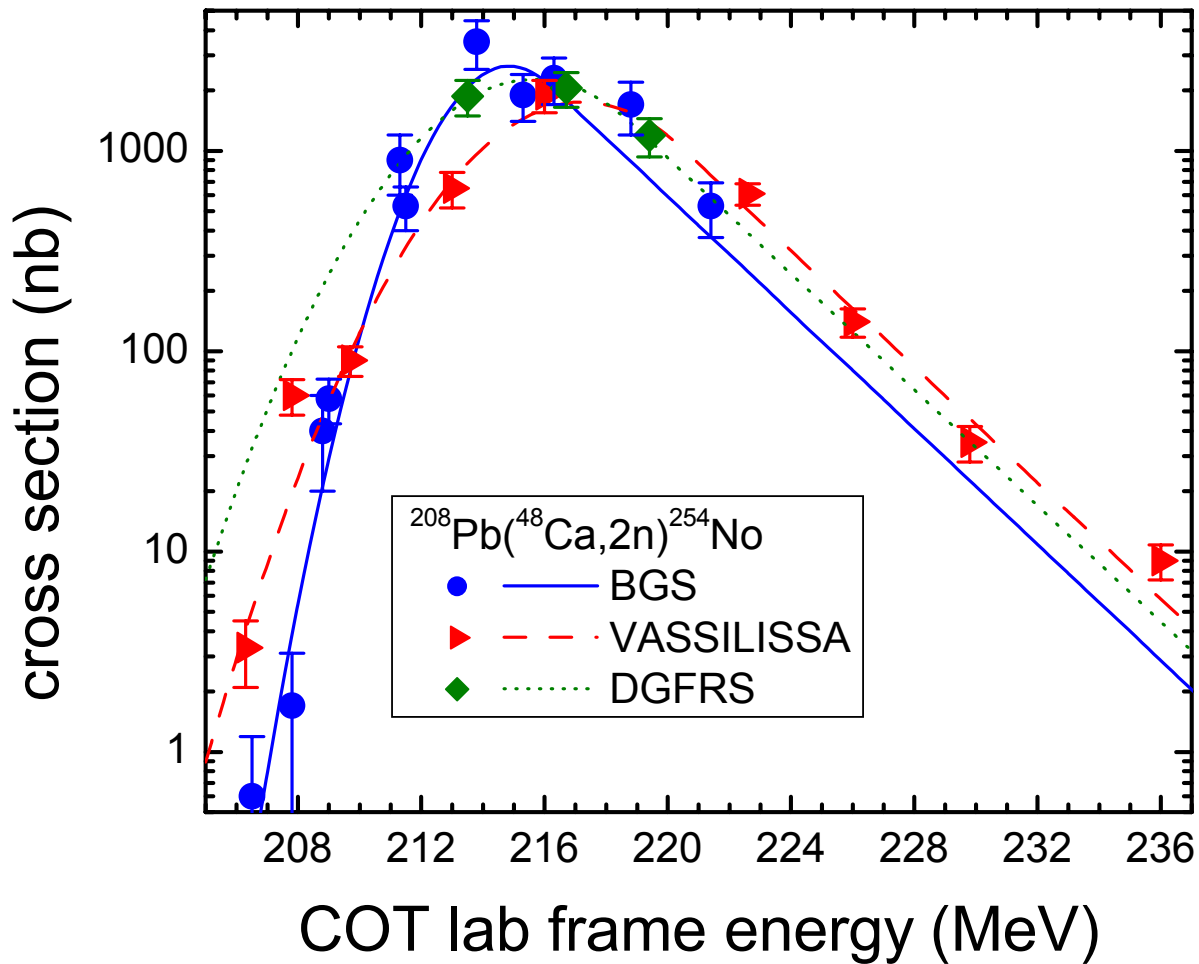


Fig. 4. $^{208}\text{Pb}(^{48}\text{Ca},2n)^{254}\text{No}$ excitation functions measured at BGS, VASSILISSA, and the DGFRS. The BGS and DGFRS centroids agree to within 1 MeV, and the amplitudes agree to within a factor of 1.2, suggesting that systematic errors in beam energy and/or separator sensitivities do not explain the discrepancies in $^{238}\text{U}(^{48}\text{Ca},3n)^{283}\text{112}$ production.